LESSONS LEARNED FROM SUPPORT DESIGN FOR CAVERNS EXCAVATED IN ROCK MASSES UNDER HIGH IN SITU STRESSES

QIAN Qihu

December 2016

Taking excavation of the underground cavern group of Jinping I Hydropower Station as the background, this presentation presents the monitoring data, numerical simulation and analysis results for deformation and failure characteristics of the surrounding rock masses.

1 Project overview and main problems encountered during construction

1 Layout of underground powerhouse

Powerhouse: length: 276.99m, span below crane beam: 25.60m, span above crane beam: 28.90m, height: 68.80m.

Transformer chamber: length: 197.10m, span: 19.30m, total height: 32.70m.

The “three generators-one chamber-one cavern” layout was adopted for the tailrace surge chamber. Two separate circular surge chambers were constructed with diameter of 34.00m and 38.00m (lower chamber) and height of 80.50m/79.50m, respectively.

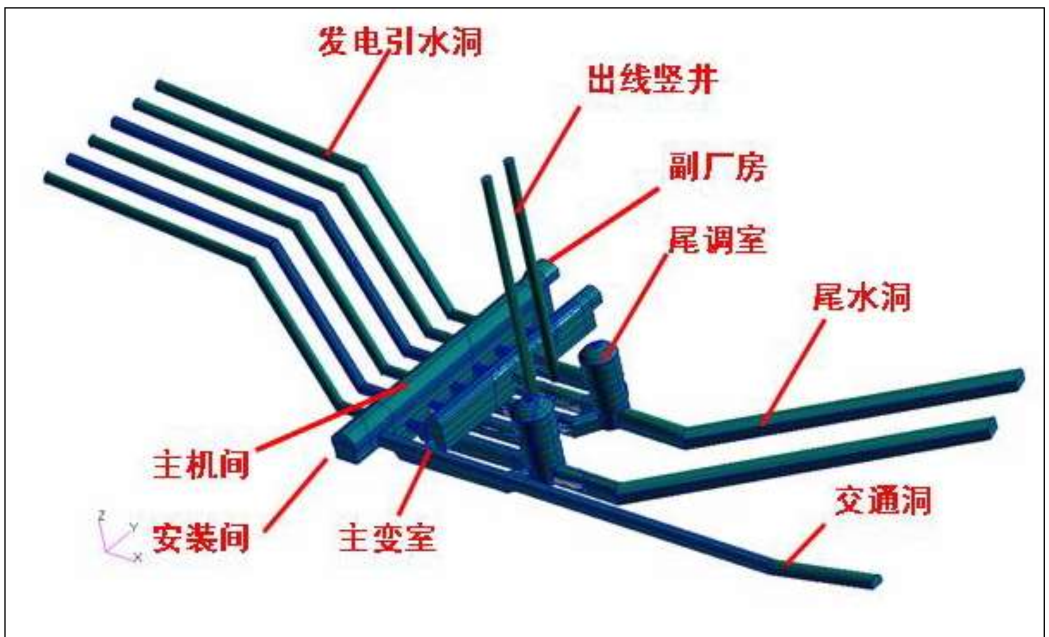

Sketch map for layout of underground cavern group of Jinping I Hydropower Station

2 Geological conditions

The geological conditions are complex at the project site. The lithology is marble intercalated with green schist. The surrounding rock mass is mainly class Ш1 rock mass, with saturated **uniaxial compressive strength Rb of 60~75MPa**.

Three large-scale NE trending faults f13, f14 and f18 are revealed at the project site. The angle between the fault strike and the axis of underground powerhouse is about 45°; greyish-green kersantite veins (X) are also developed with the fault f18, distributed at the air-conditioning room for the powerhouse, the auxiliary power house, the transformer chamber and the tailrace surge chamber. The veins are generally 2~3m wide and reach 7m in some local places. Most are of poor rock quality, belonging to class IV~V rock masses

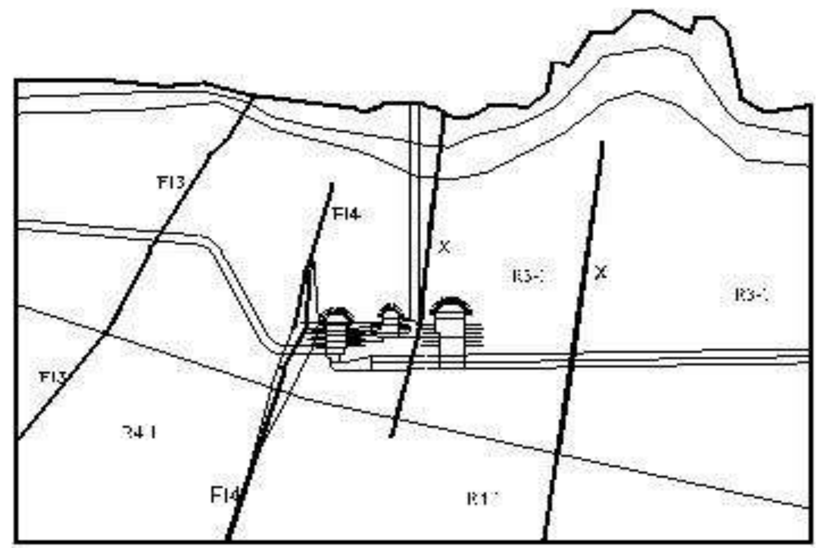

Geological profile for the underground powerhouse of Jinping I Hydropower Station

3 In situ stress condition

In situ stress tests were conducted at 16 points within the range of underground powerhouse during the feasibility study phase.

The measured maximum principal stresses: σ_1=20～35.7MPa, σ_2=10～20MPa, σ_3=4～12MPa. The orientation of σ_1 is relatively consistent between N28.5°W～N71°W, with average being N48.7°W. The angle of σ_1 is about 20~50°, with average being 34.2° ;

The strength-stress ratio is between 2~4. Regions with S≤3 are subjected to extremely high in situ stresses.

4 Problems encountered during construction

From Jan 2007 to early 2009, excavation reached the layer Ⅷ and the excavation volume was about 60% of the total excavation volume.

(1) Large deformation

The maximum deformation of the powerhouse recorded by multi-point extensometers **was about 87mm, and that of the transformer chamber was 132mm**, which were much larger than the deformation of other completely excavated caverns.

The maximum deformation at the downstream spandrel of the transformer chamber reached 200mm.

4 Problems encountered during construction

(2) Cracking of shotcrete

The rock mass revealed by excavation of the powerhouse roof was intact. However, 3-5 days after shotcreting, spalling occurred. 30 days after excavation, spalling was observed in a large range.

When the powerhouse excavation reached the layer III, the excavation depth was 22m, **cracks appeared at the downstream spandrel** near the center line of the generator group 5#.

When the powerhouse was excavated to the layer IV and the transformer chamber was excavated to the layer III, **cracks were further developed** at the downstream spandrel of the powerhouse, and extended toward the generator groups 4#, 3#, 2# and 1#, **almost appearing in the entire downstream spandrel.**

When excavation of the layer III was finished for the transformer chamber, cracking occurred in the downstream spandrel of the transformer chamber, similar to the powerhouse. **The cracks propagated from shallow depth to greater depth**.

4 Problems encountered during construction

Shotcrete cracking and distorted steel bar at the downstream spandrel of the powerhouse

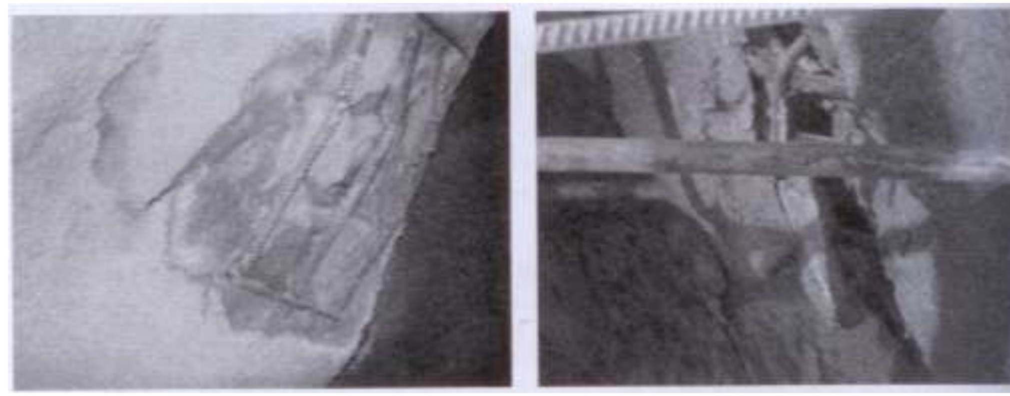

Shotcrete heave and local cracks in the downstream sidewall of the powerhouse

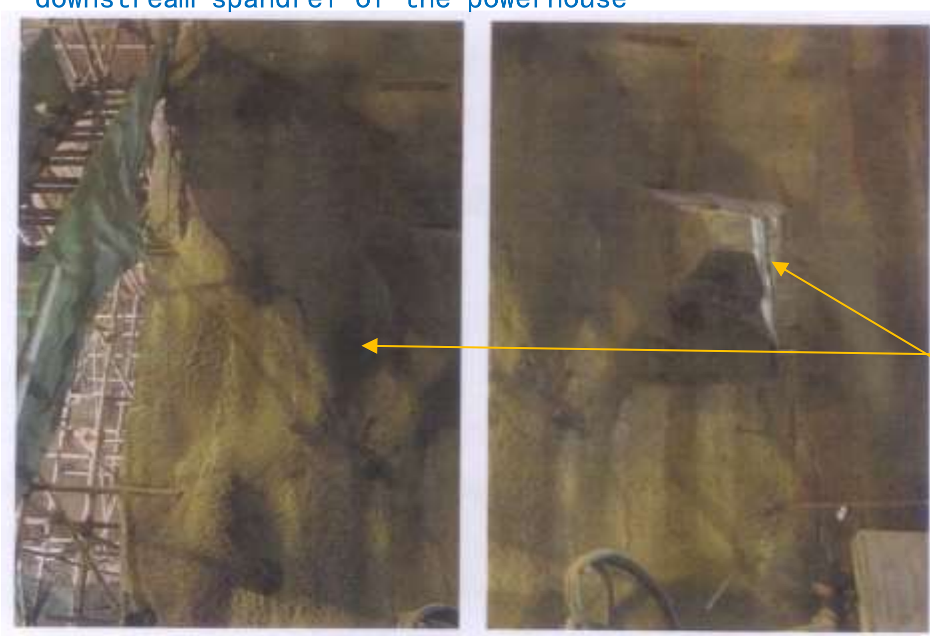

Tensile and shear cracks in the same direction between the busbar tunnel and the upstream sidewall of the transformer chamber

4 Problems encountered during construction

(3) Continuous development of loosened zones

The sound wave tests indicated that the loosened zone was developed gradually; initially, the depth was about 2m; **when excavation reached the layer III, the depth increased to 4m; when excavation reached the layers IV and V, the depth of loosened zone was more than 10m** in some local areas; **when excavation reached the layers VI and VII, the depth was more than 17m** in some local areas. **The loosened zones are discontinuous with depth**.

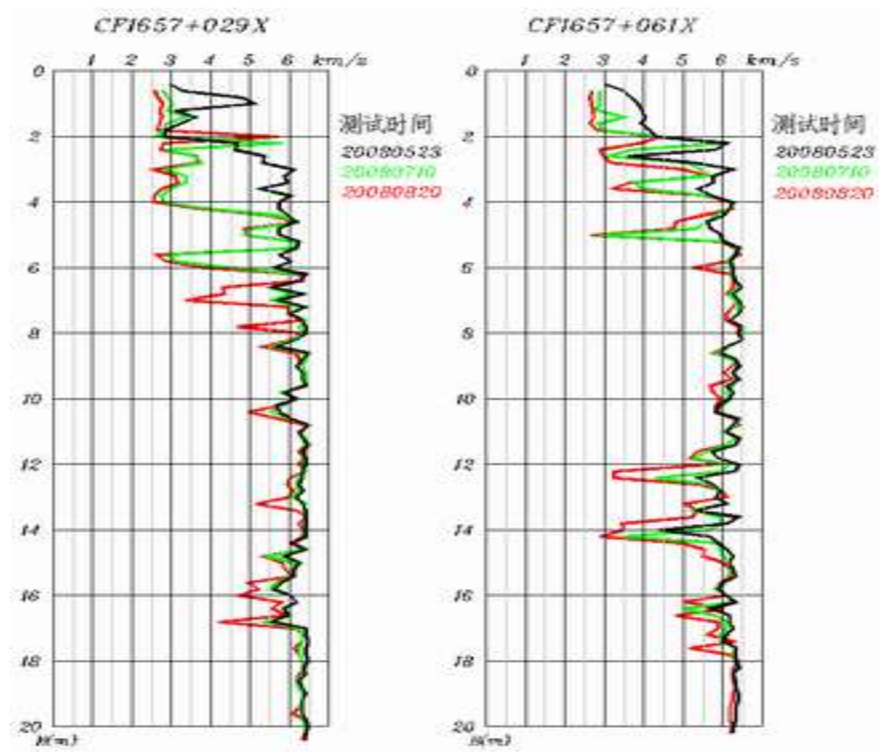

Monitoring results for loosened zones around the powerhouse

4 Problems encountered during construction

(4) Overlimit of tension in anchorage cable

In situ monitoring results indicate that: **the forces in 38.81% of the anchorage cables for the powerhouse exceeded the designed value. The maximum force even exceeded the designed value by more than 40%** (for instance, the measured force reached 266t for an anchorage cable with the deigned value of 200t; the measured force was 144t for an anchorage cable with the deigned value of 100t.)

The forces in 43.75% of the anchorage cables for the transformer chamber exceeded the designed value. The maximum force even exceeded the designed value by about 38% (for instance, the measured force reached 241t for an anchorage cable with the deigned value of 175t).

The stresses in 18.18% of rockbolts exceeded the measurement range of stress gauges in the monitoring rockbolts for the powerhouse.

2 Comparison of numerical simulation and monitoring results for deformation and damage in the surrounding rock masses

1 Numerical simulation

- The eXtended Finite Element Method (XFEM) based on the damage and fracture theory was employed. L0+126.8 and L0+31.7 sections were selected for simulation. **The displacement and stress distributions, and the internal force distribution in rockbolts and anchorage cables were simulated in the surrounding rock masses cavation reached the layer Ⅷ cavated**. The simulation results are compared with the monitoring data to verify the numerical model ;
- **The displacement and stress distributions** in the surrounding rock masses **during cavation below the layer Ⅷ were simulated**;
- **The internal force distribution in rockbolts and anchorage cables during cavation below the layer Ⅷ were simulated.** The possible failure characteristics were predicted.

1 Numerical simulation

The reason for adopting the **eXtended Finite Element Method (XFEM)** is because it can simulate the deformation and failure of the surrounding rock mass and remeshing is not required for simulating crack propagation.

The existence and propagation of cracks can be reflected by modifying the shape function. The modified shape function can be differentiated for each element. Therefore, the stiffness matrix in the XFEM is a symmetrical and sparse band matrix.

2 Numerical model (Taking Section L0+31.7 as an example)

The numerical model of the section L0+31.7 (section of the generator group 5#) is shown in the figure. The upstream sidewall of the tailrace surge chamber is close to the fault f14. With the consideration of the underground powerhouse layout, the model size is taken as 317 m×524 m.

The support in the model includes the rockbolt system, the anchorage cable system, two-ended anchors and the shorcrete layer.

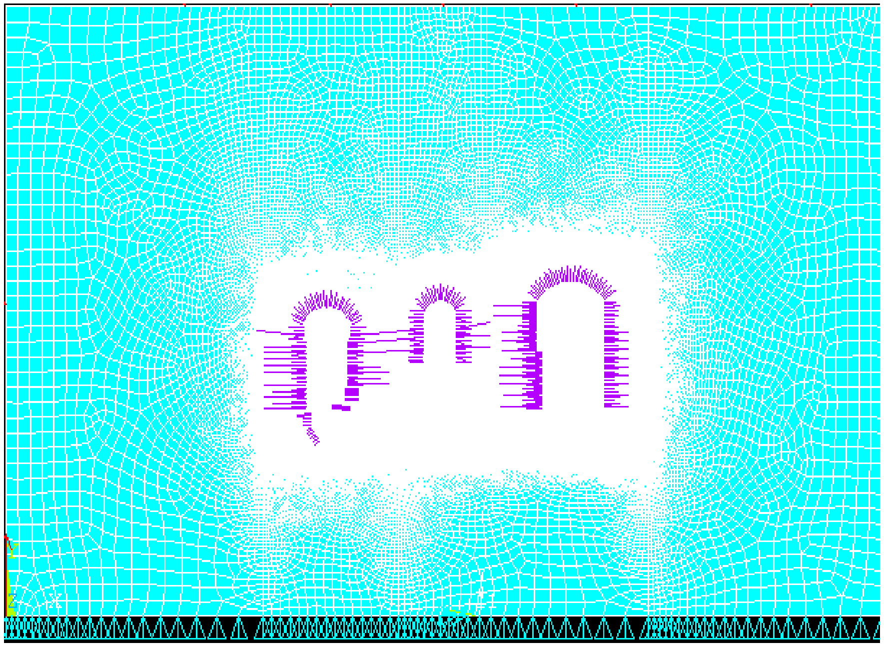

Numerical model for L0+31.7 section

3 Comparison of numerical and monitoring results for excavation from the layers Ⅰ to Ⅷ

(1) Comparison of displacement obtained by numerical modeling and monitoring (11th monthly monitoring report in 2009

Comparison of the maximum horizontal displacement

Location		Accumulative displacement recorded by multi-point extensometer (mm)	Simulation results (mm)
Powerhouse	Upstream sidewall EL1645	10.7	**136**
	Downstream sidewall EL1641	59.7	**129**
Transformer chamber	Upstream sidewall EL1660.8	10.4	**59**
	Downstream sidewall EL1664	60.9	**140**
Tailrace surge chamber No. 1	Upstream sidewall EL1666	12.44	**39**
	Downstream sidewall EL1651	——	**60**

As can be seen from the table**, the simulation results are larger than the monitoring data. The reason may be that deformation had occurred in the surrounding rock masses before the multi-point extensometer was installed, and the monitoring points were 2-6m away from the cavern wall, which didn’ t reflect the horizontal displacement of cavern wall**. However, as known from the displacement trend, both the monitoring and simulation results indicate that the downstream sidewalls of the powerhouse and transformer chamber experienced larger horizontal displacement.

3 Comparison of numerical and monitoring results for excavation from the layers Ⅰ to Ⅷ

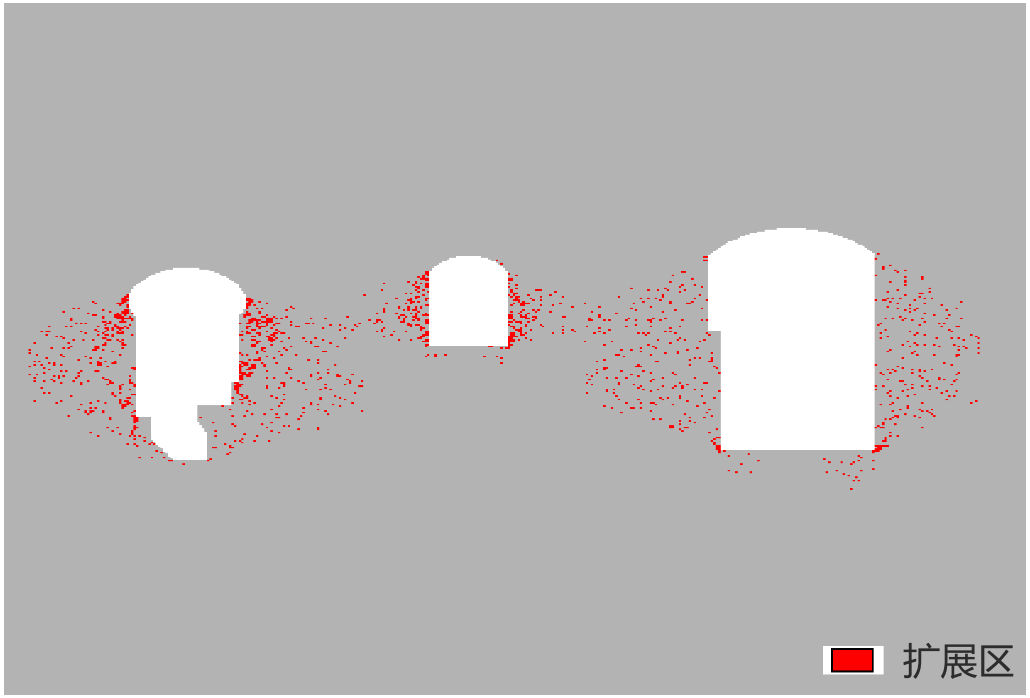

Rock fracturing zones and extension zones in Section L0+31.7

As can be seen from the figure:

1) Some cracks in the surrounding rock masses propagate and coalesce to form fractured zones. Some cracks extend without coalescence to form the extension zone. The depth of the fractured zone in the downstream sidewall of the powerhouse is about 12m, and that in the upstream sidewall of the transformer chamber is about 9m and that in the downstream sidewall of the transformer chamber is about 8m.

2) The maximum depth of the extension zone in the upstream sidewall of the powerhouse is 26m. The extension zones between the powerhouse and the transformer chamber are coalescent;

3) The extension zones between the downstream sidewall of the transformer chamber and the tailrace surge chamber are coalescent;

4) The extension zones at the roof of the powerhouse and transformer chamber are relatively small and both are smaller than 3.5m;
5) The depth of extension zone in the downstream sidewall of the tailrace surge chamber is 23m, and no fractured zone is formed;
6) Due to the horizontal tensile stresses in the sidewalls of the powerhouse and transformer chamber, splitting failure occurs in the range of 13m from the upstream sidewall of the powerhouse. Splitting failure also occurs between the powerhouse and transformer chamber, and in the range 8m away from the downstream sidewall of the transformer chamber.

The above phenomena obtained by numerical simulation are qualitatively similar and quantitatively close to the monitoring results.

3 Comparison of numerical and monitoring results for excavation from the layers Ⅰ to Ⅷ

(2) Comparison of internal forces in rockbolts and anchorage cables obtained by simulation and monitoring

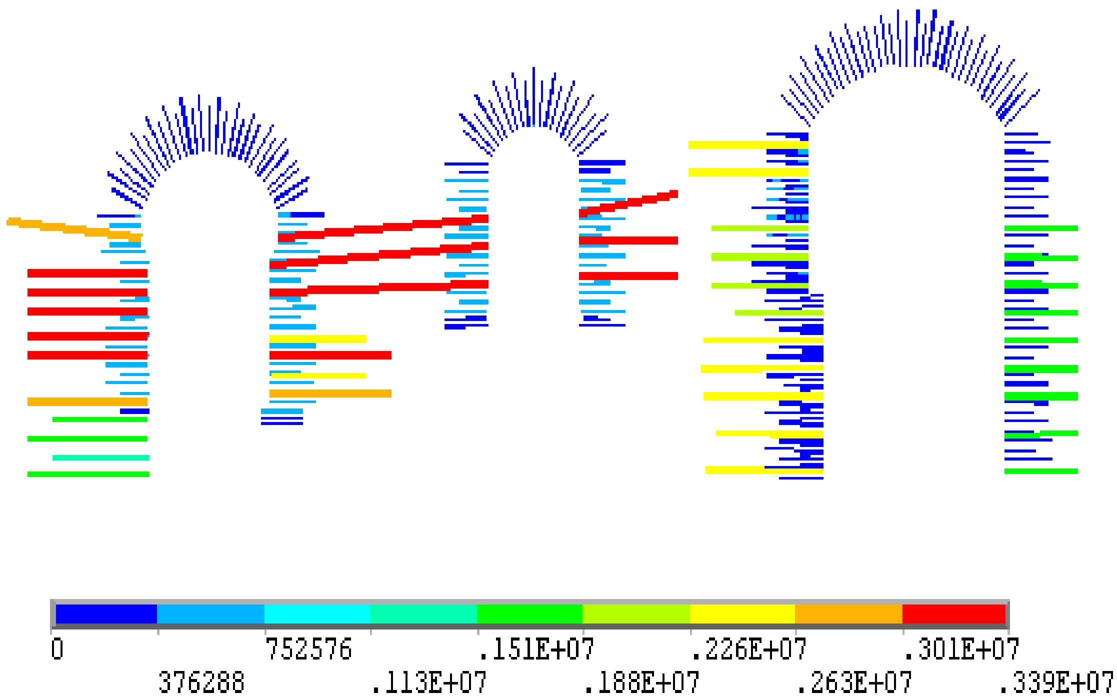

Internal force in rockbolts and anchorage cables after the layer Ⅷ was excavated for the powerhouse

4 Simulation results for layered excavation of the layers IX, X and XI

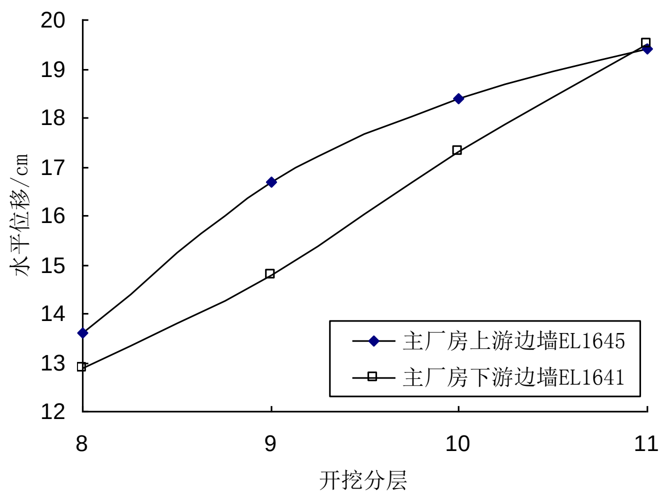

Variation of the maximum horizontal displacement of the powerhouse sidewall with excavation

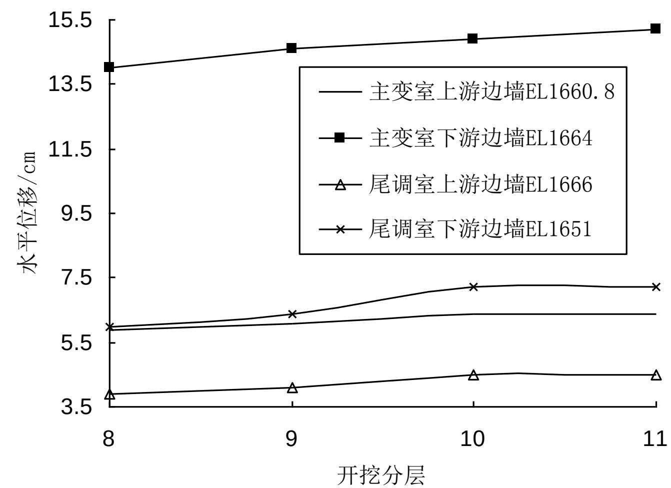

Variation of the maximum horizontal displacement in the sidewalls of the transformer chamber and the tailrace surge chamber

4 Simulation results for layered excavation of the layers IX, X and XI

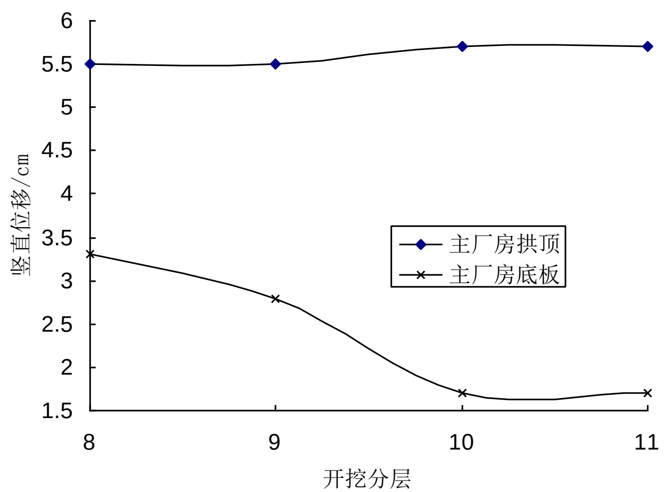

Variation of the maximum vertical displacement of the roof and floor of the powerhouse with excavation

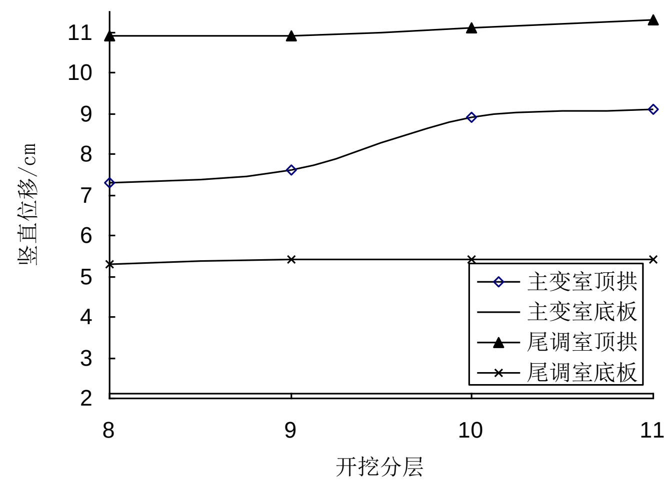

Variation of the maximum vertical displacement of the roof and floor of the transformer chamber and tailrace surge chamber with excavation

The left figure shows that, during excavation of the layers IX to XI for the powerhouse, the powerhouse roof subsided by about 0.2cm. However, as the floor width continuously decreases with excavation and the floor heave tended to be stable. In another word, excavation of the layers IX to XI for the powerhouse had little influence on the roof subsidence.

The right figure indicates that during excavation of the layers IX to XI for the powerhouse, the vertical displacement at the floor of the transformer chamber and tailrace surge chamber didn' t change much. In another word, the excavation had little influence on the vertical displacement at the floor of the transformer chamber and tailrace surge chamber. In addition, the roof of transformer chamber subsided by 1.5cm during excavation of the layers IX to XI for the powerhouse.

4 Simulation results for excavation of the layers IX, X and XI

The horizontal displacement increment at the sidewalls of underground cavern group during excavation of the layers IX–XI for the powerhouse (Unit: cm)

	Powerhouse		Transformer chamber		Tailrace surge chamber	
	Upstream sidewall	Downstream sidewall	Upstream sidewall	Downstream sidewall	Upstream sidewall	**Downstream sidewall**
Excavation of Layer IX	3.1	1.9	0.2	0.6	0.2	**0.4**
Excavation of Layer X	1.7	2.5	0.3	0.3	0.4	**0.8**
Excavation of Layer XI	**1.0**	**2.2**	**0.0**	**0.3**	**0.0**	**0.0**

The above table lists the maximum horizontal displacement increment in the sidewalls of underground cavern group during excavation of the layers IX and XI for the powerhouse. It can be seen that, due to the effect of high in situ stresses and low mechanical parameters of rock masses, the maximum horizontal displacement in the downstream sidewall of the powerhouse changed obviously and that in the sidewalls of the transformer chamber and tailrace surge chamber was relatively small.

4 Simulation results for excavation of the layers IX, X and XI

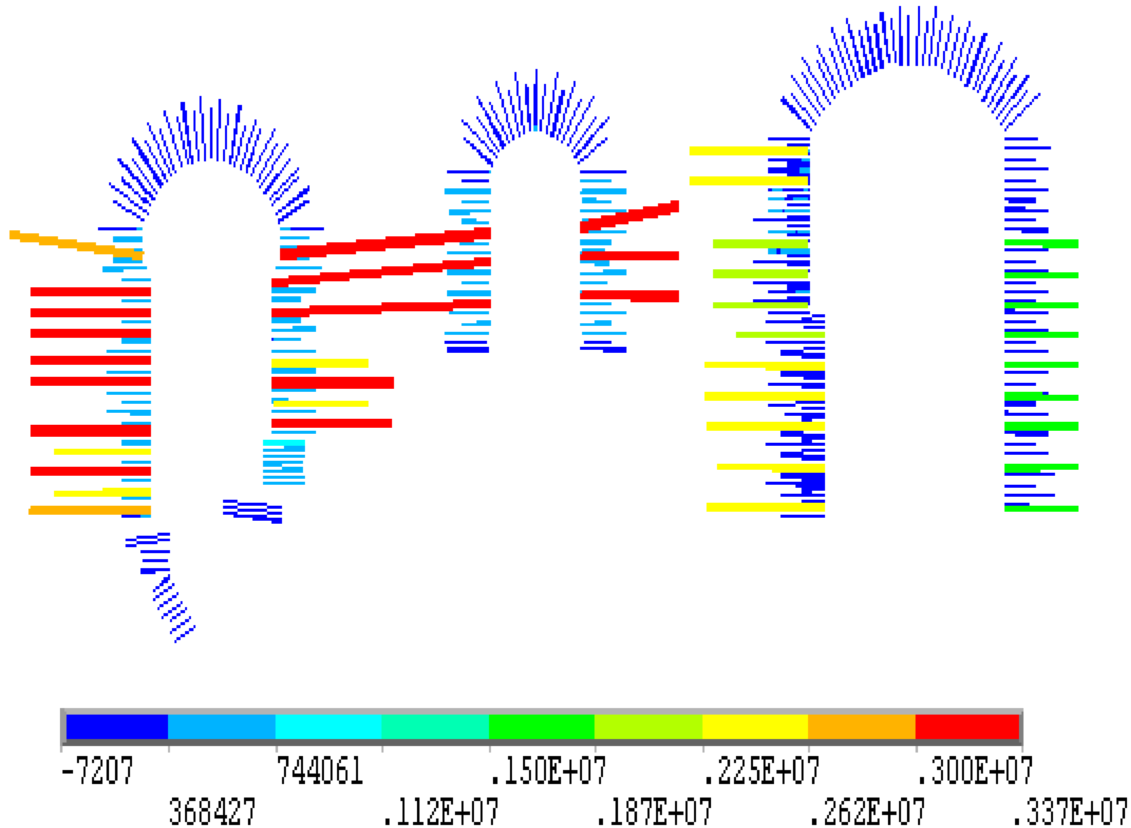

Internal forces in rockbolts and anchorage cables after the layer XI was excavated for the powerhouse

5 Comparison of numerical and monitoring results for excavation from the layers IX to XI

Summary

- Due to high in situ stresses and low rock mass parameters, **the maximum horizontal displacement in the upstream sidewall of the powerhouse will increase by 5.8cm and that in the downstream sidewall will increase by 6.6cm during excavation of the layers IX to XI for the powerhouse.** That is to say, the horizontal displacement in the downstream sidewall was greater than that in the upstream sidewall. However, the roof subsidence was small during excavation of the layers IX to XI for the powerhouse;
- Large range of vertical stress concentration occurred in the arch spring of the powerhouse, transformer chamber and tailrace surge chamber. The maximum compressive stress in the vertical direction exceeded 65MPa. Because of the vertical compressive stress concentration at the arch spring, **the rock masses near the arch spring of the three caverns may be crushed locally,** especially at the powerhouse. Due to the presence of horizontal tensile stress zone in the sidewalls of the powerhouse and transformer chamber, **splitting failure occurred in the surrounding rock masses within a distance of 15m from the upstream sidewall of the powerhouse. Splitting failure also occurred in the rock masses between the powerhouse and transformer chamber and also in the rock masses within 10m down from the downstream sidewall of the transformer chamber**.
- **The loading limit was severely exceeded in some pre-stressed anchorage cables for the powerhouse and transformer chamber.** The role restraint the surrounding rock mass of short rockbolts is not evident. Due to high in situ stresses and low rock parameters, **the axial force in some anchorage cables below the layer VIII of the upstream sidewall of the powerhouse obviously increased during excavation of the layers IX to XI for the powerhouse.**

Conclusion: According to the simulation results, the support for the surrounding rock masses needs to be further reinforced.

3 Reinforced support during construction and its effects

When excavation reached the layer Ⅷ, excavation was suspended according the suggestion of due to large deformation and severe damage. The following support measures were taken for the powerhouse, transformer chamber and tailrace surge chamber based on consultant and research:

- **Ordinary mortar-grouted rockbolts were replaced by pre-stress rockbolts** at some places for the powerhouse;
- **A few rows of 12m long pre-stressed rockbolts were added in the upstream and downstream hance and arch spring of the powerhouse and the tailrace surge chamber;**
- **A few rows of 25m long pre-stressed anchorage cables were added at some places for the powerhouse, the transformer chamber and the tailrace surge chamber;**
- **Consolidation grouting with low grouting pressure was performed at the fault f14 and the downstream arch spring.**

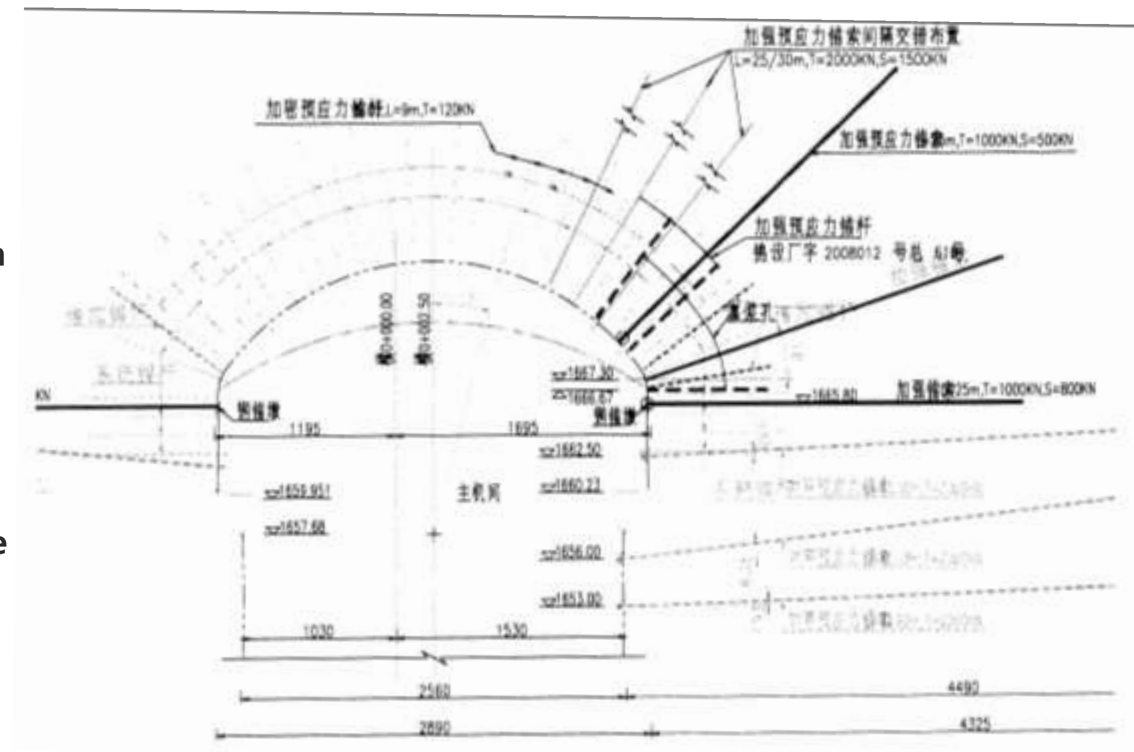

Typical cross section of reinforced support at the powerhouse spandrel

Effects of reinforced support

The monitoring data after reinforcement showed that: **The rock mass deformation was generally controllable, and the deformation recorded by multi-point extensometers tended to converge.**

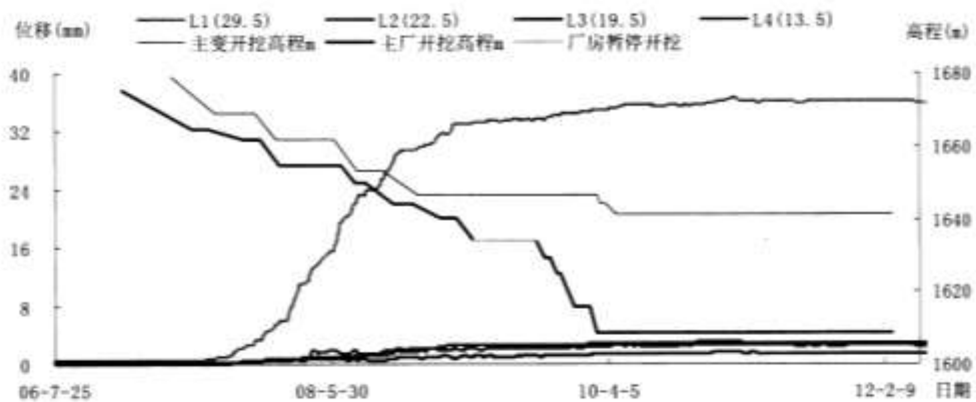

Time histories of deformation in the rock masses surrounding the powerhouse (Downstream arch spring at Sta. PL0+126, EL1670m)

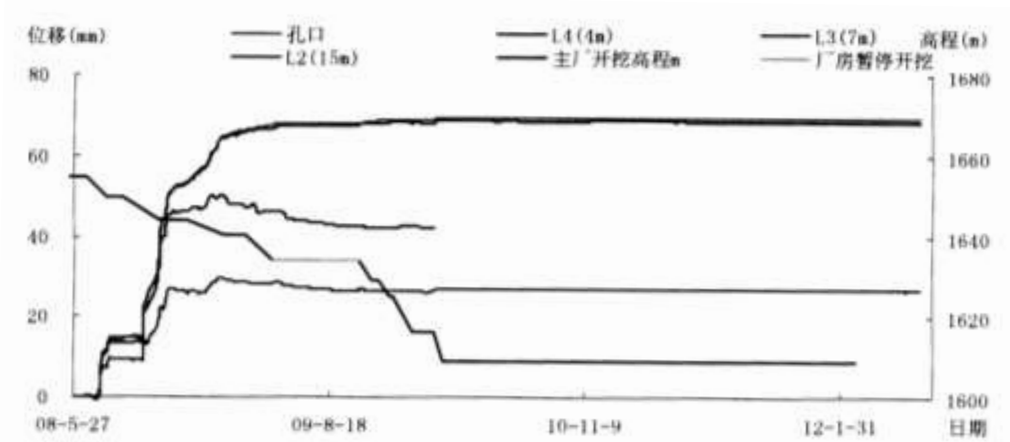

Displacement at the section 0+126.8 of the powerhouse (downstream rock anchor beam, EL1659m)

At present, all the support has been installed for excavation of underground cavern group. **The surrounding rock masses are stable and the power station is in normal operation.**

4 Causes for severe deformation and failure in the surrounding rock masses and overlimit in some anchorage cables

The root cause for severe deformation and damage in the surrounding rock mass and internal force overlimit in anchorage cables is that the original design cannot adapt to the rock deformation and failure characteristics of the highly stressed rock masses (strong compression) subjected to excavation unloading.

Strong compression in the surrounding rock masses is caused by the gravity of the overlying rock masses and high in situ stresses resulted from tectonic movement. Whether the in situ stress is high or low is relative to the uniaxial compressive strength (UCS) of the rock mass. The in situ stresses in the surrounding rock masses of underground powerhouse of Jinping I Hydropower Station mostly exceed half of the UCS, belonging to extremely high in situ stresses or strong compression.

During cavern excavation in rock masses subjected to high in situ stresses, the high in situ stresses at the cavern boundaries are relieved. The three effects of excavation unloading are gradually transferred from the surface to deeper rock masses:

(1) Effect of radial tensile stress

The tensile effect (tensile wave) is transferred to the deeper rock masses after excavation. As the radial stress at the excavation face is zero and the geostresses in the deeper rock masses are high, displacement occurs at a certain rate along the radial direction, leading to tensile strain in the rock masses. When the strain exceeds the tensile strain limit, tensile failure occurs. If the in situ stresses are high, the gradient of the radial stress is great and the displacement rate is high. If a certain speed remains after rock mass failure, "rockburst" occurs.

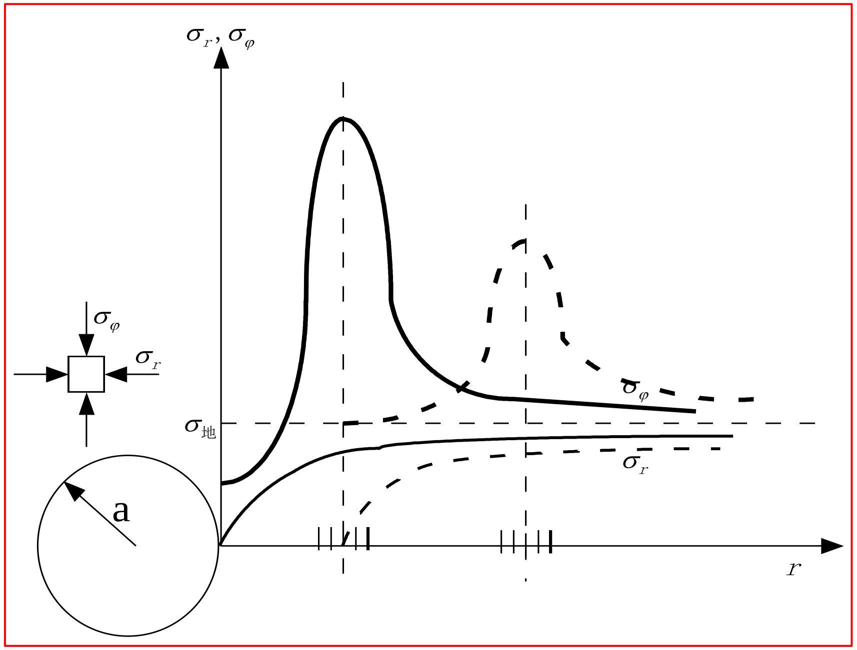

(2) Effect of abutment stress wave due to transfer of abutment stress

Excavation results in stress concentration at the cavern boundaries. Subsequently, the rock masses at the boundaries have to bear even higher circumferential stresses, similar to the abutment. Therefore, it is called the abutment stress zone. The abutment stress zone in rock masses subjected to initial strong compression (high in situ stress) can easily lead to rock mass failure due to the combined effect of high circumferential compressive stresses and radial tensile stresses caused by stress concentration. The failed rock masses can no longer sustain the high circumferential compressive stresses due to stress concentration (also called the hump stress). The abutment stress zone gradually transfers into the deeper rock masses, leading to the abutment stress wave effect towards the deeper rock masses.

(3) Effect of pseudo free surface transfer

The excavation boundary is a free surface. The cracks due to the effect of radial tensile stress and the abutment stress zone form a new free surface, where stress relief and unloading occur. In order to differentiate from the original free surface, the newly formed surface is called the pseudo free surface. A new stress concentration zone (the abutment stress zone) will form at the pseudo free surface. If the initial geostresses are high, a new failure zone will be formed……. Eventually, the second or third failure zone and pseudo free surface gradually transfer towards the deeper rock masses.

In summary, the three effects due to excavation unloading in highly stressed rock masses lead to continuous failure transfer towards the deeper rock masses. Different from rock projects in shallow depth or low in situ stress zone which have only one yielding and relaxation zone around the cavern, rock fracturing occurs in multiple zones, which is called **the zonal fracturing phenomenon**. Therefore, the rock deformation and failure in the rock masses around caverns in highly stressed zones is much more severe than that for shallow rock projects subjected to low stresses. Continuous transfer of deformation and failure towards the deeper rock masses is the rheological characteristics of rock masses, which is also the **rock mass rheology** in the residual stress zone mentioned by Professor Tan Tjong-kie.

The above analysis is conducted for excavation of a single cavern under two-dimensional high in situ stress unloading. Excavation of underground powerhouse of Jinping I Hydropower Station is more complex as it involves three-dimensional excavation unloading of the powerhouse, the transformer chamber and the busbar tunnel and cutting of multiple faults including F1, F18 and F13 etc. The rock mass deformation and failure is more severe.

For the above-mentioned cavern excavation in highly stressed rock masses, proper support measures have to be taken in order to prevent large deformation and failure, severe overlimit in rockbolts and anchorage cables. Engineering practices in this project indicate that the original design based on continuum mechanics analysis, with which rock mass failure occurred when excavation reached the layer Ⅷ, is no longer applicable.

5 General laws of 2D zonal fracturing phenomenon due to excavation unloading in highly stressed rock masses

Based on site investigation, analog tests in laboratory, theoretical studies and numerical analyses on the zonal fracturing phenomenon in highly stressed rock masses, it is shown that:

- The higher the in situ stress $\sigma_{地}$ relative to the uniaxial compressive strength, i.e., $\sigma_{地}/\sigma_{压}$, the greater the number of fracturing zones, and the more severe rock deformation and failure.
- The higher the horizontal in situ stress relative to the vertical in situ stress, the greater the number of fracturing zones, and the more severe rock deformation and failure.
- The higher the tunnel and cavern excavation speed, i.e., the more rapid the unloading, the greater the number of fracturing zones, and the more severe rock deformation and failure.
- The greater the number of primary joints in the rock masses, the greater the number of fracturing zones, and the more severe rock deformation and failure. In another word, the primary joints have important effects on the shape and distribution of fracturing zones.

6 Suggestions on support and reinforcement for excavation in rock masses under high in situ stresses

In light of the causes and mechanism of severe deformation and damage in the surrounding rock masses, the following support and reinforcement measures are suggested for underground cavern excavation for the hydropower station:

- The cavern shall be excavated in layers and sections, so as to reduce the unloading speed, mitigate stress concentration, and slow down the transfer of stress concentration zones and abutment stress zones towards the deeper rock masses;

- Reinforcement measures shall be applied immediately after excavation. That is, with excavation in layers and sections, reinforcement measures (including grouting, rockbolts and anchorage cables) shall be implemented in layers and sections, so as to enhance the rock mass strength before failure, and slow down the transfer of the abutment stress and pseudo free surface towards the deeper rock masses. Subsequently, it can reduce zonal fracturing, deformation and failure of the surrounding rock masses;

- The anchorage length or the anchored section shall reach the unfractured zone behind the farthest fracturing zone; Grouting shall reach all the fracturing zones. Grouting and anchorage shall be in place as early as possible. Grouting shall be performed in two steps with gradually increasing pressure so as to adapt to the actual condition after crack propagation. Second grouting shall be performed for the areas with displacement non-convergence so as to improve rock strength and speed up convergence. However, the grouting pressure shall be well controlled. The internal force in anchorage cables shall be monitored during grouting, so as to avoid damage to anchorage cables;
- The pressure-diffusing-type anchorage cables shall be adopted. The number of anchorage sections shall be determined the quantity of fracturing zones, i.e., one anchorage section for each fracturing zone. The anchored sections shall be located in unfractured zone or microfractured zone the between the fractured zones.
- The rockbolt should reach the area behind the first fracturing zone. The fracturing zones can be detected by borehole exploration or ultrasonic device.

7 Lessons learnt from rock deformation and failure during excavation of underground cavern group for Jinping I Hydropower Station

1. **The combined effects of excavation unloading in rock masses subjected to high in situ stresses lead to rock failure and gradual transfer into deeper rock masses, leading to formation of fracturing zones.** Zonal fracturing generally occurs in deep rock masses. It may also occur in some relatively shallow locations, for instance, the underground cavern group of Jinping I Hydropower Station. It is different from excavation of shallow rock masses, where only one large yielding zone is formed around the cavern and may not results in rock failure.

2. **The traditional elasto-plastic mechanics theory only analyzes whether the rock mass reaches yielding strength, without considering rock mass damage and evolution, i.e., crack initiation, propagation and coalescence.** Therefore, it is only applicable for analyzing rock deformation for excavation at shallow depth, and not applicable for severe rock deformation and failure during excavation of deep rock masses subjected to high in situ stresses, i.e., the zonal fracturing phenomenon

3. **Rock mass stability analysis and support design must be based on the theory applicable for analyzing rock deformation and failure. The DDA method, the extended finite element method, the generalized particle dynamics, the non-Euclidean model and the strain gradient theory can be applied to analyze deformation and failure of rock masses under high in situ stresses.**

Thanks !